

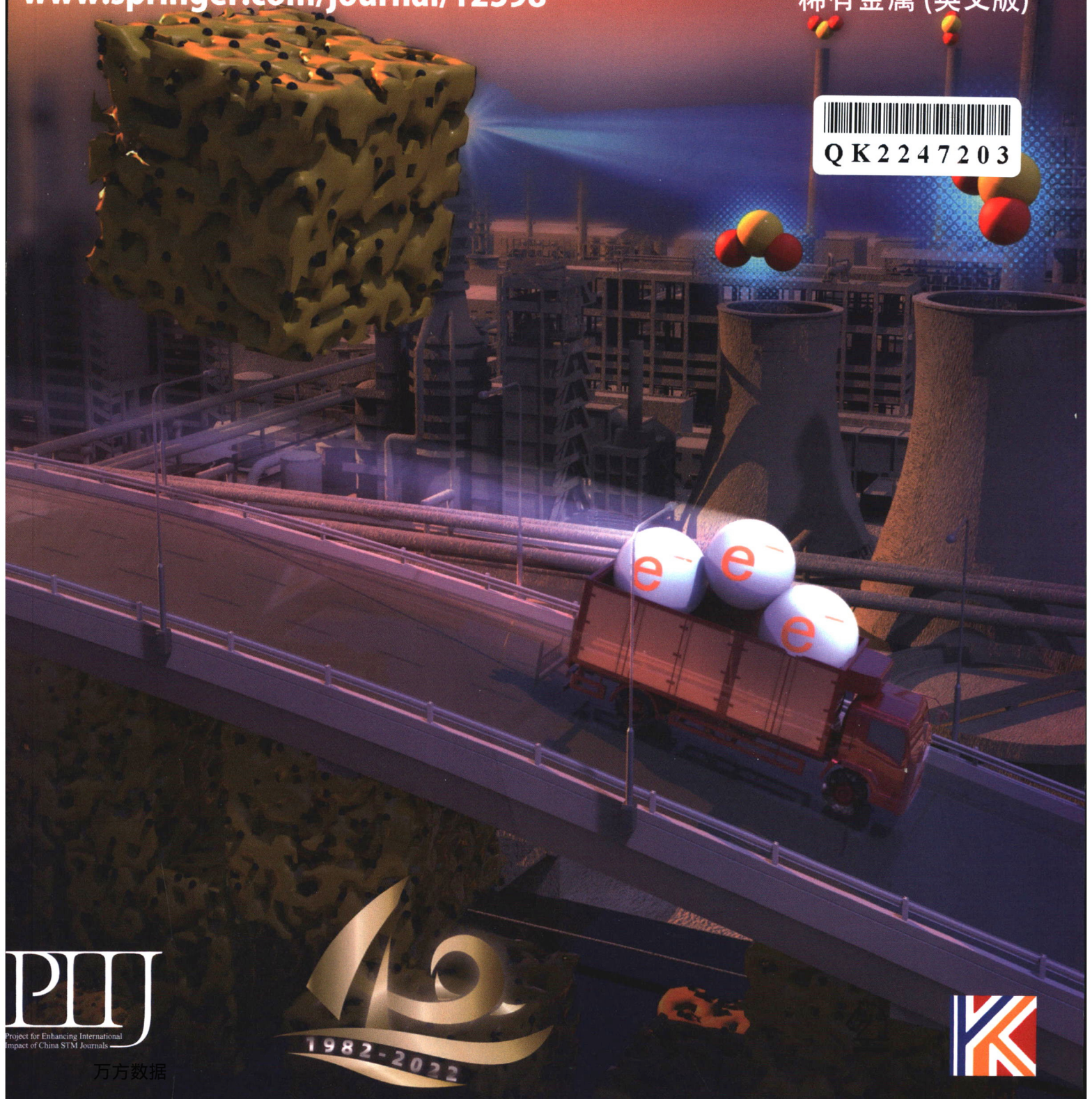
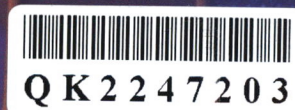
ISSN 1001-0521 · e-ISSN 1867-7185
CN 11-2112/TF · CODEN RARME 8

Volume 41 · Number 11 · November 2022

RARE METALS

www.springer.com/journal/12598

稀有金属 (英文版)



PEIJ
Project for Enhancing International
Impact of China STM Journals

万方数据



MINI REVIEWS

Self-assembly of nanoparticles at solid–liquid interface for electrochemical capacitors
X. Li · C. Chen · Q. Niu · N.-W. Li · L. Yu · B. Wang 3591

Flexible carbon fiber-based composites for electromagnetic interference shielding
H.-Y. Zhang · J.-Y. Li · Y. Pan · Y.-F. Liu · N. Mahmood · X. Jian 3612

LETTERS

In situ construction of a favorable cathode electrolyte interphase through a fluorosilane additive for high-performance Li-rich cathode materials
Y.-Y. Pan · C.-D. Qiu · S.-J. Qin · Z.-F. Wang · J.-S. Yang · H.-J. Cong · F.-S. Ke 3630

Stabilized cathode/sulfide solid electrolyte interface via Li_2ZrO_3 coating for all-solid-state batteries
C. Zhao · Z.-Q. Liu · W. Weng · M. Wu · X.-Y. Yan · J. Yang · H.-M. Lu · X.-Y. Yao 3639

Revealing layer-dependent interlayer interactions by doping effect on graphene in WSe_2/N -layer graphene heterostructures using Raman and photoluminescence spectroscopy
Y.-B. Shan · X.-F. Yue · J.-J. Chen · J.-K. Han · G. Ekoya · L.-G. Hu · R. Liu · Z.-J. Qiu · C.-X. Cong 3646

Value-added formate production from selective ethylene glycol oxidation based on cost-effective self-supported MOF nanosheet arrays
L. Jiao · W. Wei · X. Li · C.-B. Hong · S.-G. Han · M.I. Khan · Q.-L. Zhu 3654

Synergistic effect of cubic $\text{C}_3\text{N}_4/\text{ZnO}/\text{C}$ hybrid composite for selective detection of sulfur dioxide
X.-J. Miao · X.-J. Zhao · H. Qin · Q. Jin · Y. Chen · Z.-Q. Cao · W.-T. Yang · Q.-J. Wang · Q.-H. Pan 3662

High uniformity and stability of 1S1R directly stacked for high-density cross-point memory applications
Z.-Y. Yu · J.-Y. Zhao · G.-K. Ma · A. Chen · D.-L. Chen · Y.-H. Rao · H. Wang 3671

Molecular dynamics study on microscale residual stress of graphene/aluminum nanocomposites by selective laser sintering
X.-N. Hao · X. Liu 3677

High specific surface area inherited from sea-urchin-like AACH clusters prepared by a novel spray precipitation
X.-Y. Zhang · L. Zhang · T.-Y. Zhou · B.-H. Sun · S. Wei · Y.-F. Cao · M.-Y. Liu · P.-F. Sang · C. Wei · W. Chen · H. Chen 3684

ORIGINAL ARTICLES

In situ polymerization of 1,3-dioxolane infiltrating 3D garnet framework with high ionic conductivity and excellent interfacial stability for integrated solid-state Li metal battery
L.-H. Chen · Z.-Y. Huang · S.-L. Chen · R.-A. Tong · H.-L. Wang · G. Shao · C.-A. Wang 3694

Porous carbon nanofibers derived from low-softening-point coal pitch towards all-carbon potassium ion hybrid capacitors
G.-Y. Wang · X.-H. Wang · J.-F. Sun · Y.-M. Zhang · L.-R. Hou · C.-Z. Yuan 3706

Highly flexible, mechanically strengthened metallic glass-based composite electrode with enhanced capacitance and cyclic stability
Y. Xu · P.M. Yiu · Y.-K. Wang · X.-M. Qin · T. Shibayama · S. Watanabe · M. Ohnuma · D.-Z. Chen · H. Cheng · C.-H. Shek · Z.-G. Lu · C. Liu 3717

Deciphering $\text{H}^+/\text{Zn}^{2+}$ co-intercalation mechanism of MOF-derived 2D MnO/C cathode for long cycle life aqueous zinc-ion batteries
Z.-X. Zhu · Z.-W. Lin · Z.-W. Sun · P.-X. Zhang · C.-P. Li · R. Dong · H.-W. Mi 3729

Enhanced performance of core–shell structured sodium manganese hexacyanoferrate achieved by self-limiting Na^+/Cs^+ ion exchange for sodium-ion batteries
Y.-D. Guo · J.-C. Jiang · J. Xie · X. Wang · J.-Z. Li · D.-H. Wang · A.-J. Zhou 3740

High-capacity potassium ion storage mechanisms in a soft carbon revealed by solid-state NMR spectroscopy
J.-H. Han · J. He · Q.-Y. Zou · J. Zhang · Z. Yang · Z.-W. Zhao · H.-X. Chen · H.-J. Yue · D.-W. Wang · H.-C. Lin · H.-D. Liu · G.-M. Zhong · Z.-Q. Peng 3752

Poly(m-phenylene isophthalamide)-reinforced polyethylene oxide composite electrolyte with high mechanical strength and thermostability for all-solid-state lithium metal batteries
Y.-N. Liu · Z. Xiao · W.-K. Zhang · J. Zhang · H. Huang · Y.-P. Gan · X.-P. He · G.G. Kumar · Y. Xia 3762

Silicon-carbide fiber-reinforced polymer electrolyte for all-solid-state lithium-metal batteries
W.-Q. Wei · B.-Q. Liu · Y.-Q. Wang · K. Yan · H. Zhang · Y.-S. Qi 3774

Mechanism exploration of enhanced electrochemical performance of single-crystal versus polycrystalline $\text{LiNi}_{0.8}\text{Mn}_{0.1}\text{Co}_{0.1}\text{O}_2$
T.-Y. Zeng · X.-Y. Zhang · X.-Y. Qu · M.-Q. Li · P.-P. Zhang · M.-R. Su · A.-C. Dou · A. Naveed · Y. Zhou · Y.-J. Liu 3783

Graphene oxide as a hole extraction layer loaded on BiVO₄ photoanode for highly efficient photoelectrochemical water splitting
M.-L. Guo · S.-P. Wan · C.-L. Li · K. Zhang 3795

Investigation on halogen-doped n-type SnTe thermoelectrics
C.-R. Guo · B.-C. Qin · D.-Y. Wang · L.-D. Zhao 3803

Domain wall dynamics driven by a circularly polarized magnetic field in ferrimagnet: effect of Dzyaloshinskii–Moriya interaction
T.-T. Liu · Y.-F. Hu · Y. Liu · Z.-J.-Y. Jin · Z.-H. Tang · M.-H. Qin 3815

Tailoring perpendicular magnetic anisotropy in Co/Pt multilayers by interface doping with ultrathin Fe layer
X. Chen · S.-L. Jiang · D.-W. Wang · K. Yang · J.-H. Lu · G.-H. Yu 3823

Ultrasensitive and accurate diagnosis of urothelial cancer by plasmonic AuNRs-enhanced fluorescence of near-infrared Ag₂S quantum dots
D. Zhang · C.-P. Ding · X.-Y. Zheng · J.-Z. Ye · Z.-H. Chen · J.-H. Li · Z.-J. Yan · J.-H. Jiang · Y.-J. Huang 3828

A cluster-plus-glue-atom composition design approach designated for multi-principal element alloys
X. Liu · H.-B. Ke · L. Wang · Y.-J. Liang · L.-J. Wang · B.-P. Wang · L. Wang · Q.-B. Fan · Y.-F. Xue 3839

Electrophoretic deposition of chitosan–bioglass[®]–hydroxyapatite–halloysite nanotube composite coating
A. Molaie · M. Yousefpour 3850

Hexagonal packing lattice formed by functionalized gold nanoparticles
X.-B. Mang · L.-Q. Yao 3858

Intergranular corrosion of spark plasma sintered 2024 aluminum alloy at different heat treatment states
Y.-B. Meng · S.-M. Li · J.-H. Liu · M. Yu · W.-M. Tian 3865

Plastic deformation of magnesium alloy with different forming parameters during ultrasonic vibration-assisted single-point incremental forming
C.J. Su · T.T. Xu · K. Zhang · K. Zhang · S.M. Lou · Q. Wang 3878

Cube texture evolution of Ni5W alloy substrates and La–Zr–O buffer layer of YBCO-coated conductors
P. Wang · H. Tian · H.-L. Suo · C. Ren · Y.-R. Liang · L. Ma · M. Liu 3887

High-temperature oxidation behavior of HVOF-sprayed rare earth-modified WC–12Co coating
Z.-Q. Hang · N.-Y. Xi · Y. Liu · Y. Liu · H. Chen 3895

An analytical approach to modeling stress–strain relationship of particle–reinforced metal matrix composites
Z.-B. Xiang · J.-H. Nie · S.-H. Wei · T. Zuo · J.-Z. Fan 3903

Microstructures and mechanical properties of Cu/Al compound materials during thermal cycle
B. Wang · P. Liu · X.-K. Liu · Z.-Y. Wang · Y.-Y. Wang · X.-H. Chen · X.-Z. Liu 3911

Flotation separation of spodumene and albite with activation of calcium ion hydrolysate components
X.-P. Luo · Y.-B. Zhang · H.-P. Zhou · F.-X. Xie · Z.-Z. Yang · B.-Y. Zhang · C.-G. Luo 3919

High-temperature synthesis and electronic bonding analysis of Ca-doped LaMnO₃ rare-earth manganites
N. Thenmozhi · R. Saravanan 3932

Cover Picture

X.-J. Miao et al. Synergistic effect of cubic C₃N₄/ZnO/C hybrid composite for selective detection of sulfur dioxide

Further articles can be found at link.springer.com

Instructions for Authors for *Rare Met.* are available at www.springer.com/12598

RARE METALS (Monthly)

Volume 41 • Number 11 • November 2022

Cover story

(Xin-Jia Miao, Xiao-Jun Zhao, Hao Qin, Qi Jin, Yang Chen, Zong-Qiang Cao, Wei-Ting Yang, Qing-Ji Wang, Qin-He Pan, pp. 3662–3670)

Synergistic effect of cubic C₃N₄/ZnO/C hybrid composite for selective detection of sulfur dioxide

With the progress of human society and the development of industry, much attention has been focused on the detection of harmful gases in indoor and outdoor environments. SO₂, which is a colorless and highly toxic gas, is harmful to the environment and human health. It is necessary to develop gas sensing materials with good selectivity and durability to SO₂. A C₃N₄/ZnO/C hybrid, MFM@IRMOF-3-T, was prepared successfully for SO₂ monitoring by annealing the composite of melamine formaldehyde resin microsphere (MFM) and IRMOF-3. Its excellent sensing response, selectivity and repeatability can be attributed to the formation of C₃N₄ during the annealing process, which improves the electrical conductivity of the annealed product, and the bonding of nitrogen in MFM and zinc in IRMOF-3, which promotes electron transfer in MFM@IRMOF-3-T. The study of the C₃N₄/ZnO/C hybrid provides an effective strategy for the preparation of SO₂ sensor derived from MOF-based composite.

Edited and Published by Youke Publishing Co., Ltd.

(No. 2, Xijiekouwai Str., 100088 Beijing, China)

Tel.: +86 10 82241917; Fax: +86 10 82240869

Email: raremetals@grinm.com

Administrator: China Association for Science and Technology

Sponsor: The Nonferrous Metals Society of China

GRINM Group Co., Ltd.

Printer: Beijing Shengpinfengshang Technology Development Co., Ltd.,
Beijing, China

万方数据

ISSN 1001-0521



9 771001 052220

Price: RMB 300